SCIENTIFIC REPORTS

OPEN

Improve oxidation resistance at high temperature by nanocrystalline surface layer

Received: 25 November 2014
Accepted: 15 July 2015
Published: 13 August 2015

Z. X. Xia[1], C. Zhang[2], X. F. Huang[3], W. B. Liu[2] & Z. G. Yang[2]

An interesting change of scale sequence occurred during oxidation of nanocrystalline surface layer by means of a surface mechanical attrition treatment. The three-layer oxide structure from the surface towards the matrix is Fe_3O_4, spinel $FeCr_2O_4$ and corundum $(Fe,Cr)_2O_3$, which is different from the typical two-layer scale consisted of an Fe_3O_4 outer layer and an $FeCr_2O_4$ inner layer in conventional P91 steel. The diffusivity of Cr, Fe and O is enhanced concurrently in the nanocrystalline surface layer, which causes the fast oxidation in the initial oxidation stage. The formation of $(Fe,Cr)_2O_3$ inner layer would inhabit fast diffusion of alloy elements in the nanocrystalline surface layer of P91 steel in the later oxidation stage, and it causes a decrease in the parabolic oxidation rate compared with conventional specimens. This study provides a novel approach to improve the oxidation resistance of heat resistant steel without changing its Cr content.

9% Cr martensitic heat resistant steels such as P91 steel have been considered as the primary candidate structural materials for advanced fossil fired power plants and generation IV nuclear power plants. Due to long-term exposures to high temperatures, the high temperature creep resistance and high temperature oxidation resistance of P91 steel should be simultaneously improved. A Cr content of around 9 wt% in martensitic heat resistant steels is required for the optimization in creep properties, and creep resistances of 9Cr heat resistant steels could be further improved by the control of precipitation behaviors[1,2]. It is reported that increasing the Cr content in excess of about 12 wt% is effective in inhibiting the growth of oxide scale for martensitic heat resistant steels[3]. Some researchers even suggest Cr-enriched $(Fe,Cr)_2O_3$ protective scale could form on surface layer of the heat resistant steels with Cr content in excess of 17 wt%[4,5]. With increasing Cr content, the oxidation resistance would be improved obviously in heat resistant steels. However, the Cr content in excess of 12 wt% will induce the formation of δ ferrite, which is detrimental to mechanical properties, Therefore, traditional techniques and methods such as improving Cr content hardly resolve the contradictions of the component requirement between creep resistance and oxidation resistance in martensitic heat resistant steels. Grain refinement is an advantageous approach, to increase the oxidation resistance of heat resistant steels in steam without the necessity of increasing the alloy Cr content[6]. Fortunately, if only the microstrcture in the surface layer is refined at the nanometer scale by mean of a surface mechanical attrition treatment (SMAT),which may increase the oxidation resistance of heat resistant steels, the negative effect of the nanocrystalline surface layer on mechanical properties can been neglected[7].

The nanocrystalline structure with a large number of grain boundaries, which can act as fast atomic diffusion channels[8,9]. Compared to diffusions in materials with conventional grain sizes, greatly enhanced atomic diffusivities have been reported in nanocrystalline materials[10,11]. Hence, it is expected that SMAT, which can produce nanocrystalline layer on the surface of steels, can significantly improve oxdiation resistance. In the present work, the high temperature oxidation behavior of nanocrystallined P91 steal is studied, and effect of nano-grain boundary on the formation of oxide scale is illustrated, all of which can

[1]Shagang School of Iron and Steel, Soochow University, Suzhou, 215021, China. [2]School of Materials Science & Engineering, Tsinghua University, Beijing, 100084, China. [3]College of Materials Science and Engineering, Sichuan University, Chengdu, 610065, China. Correspondence and requests for materials should be addressed to Z.X.X. (email: xiazhixin2000@163.com)

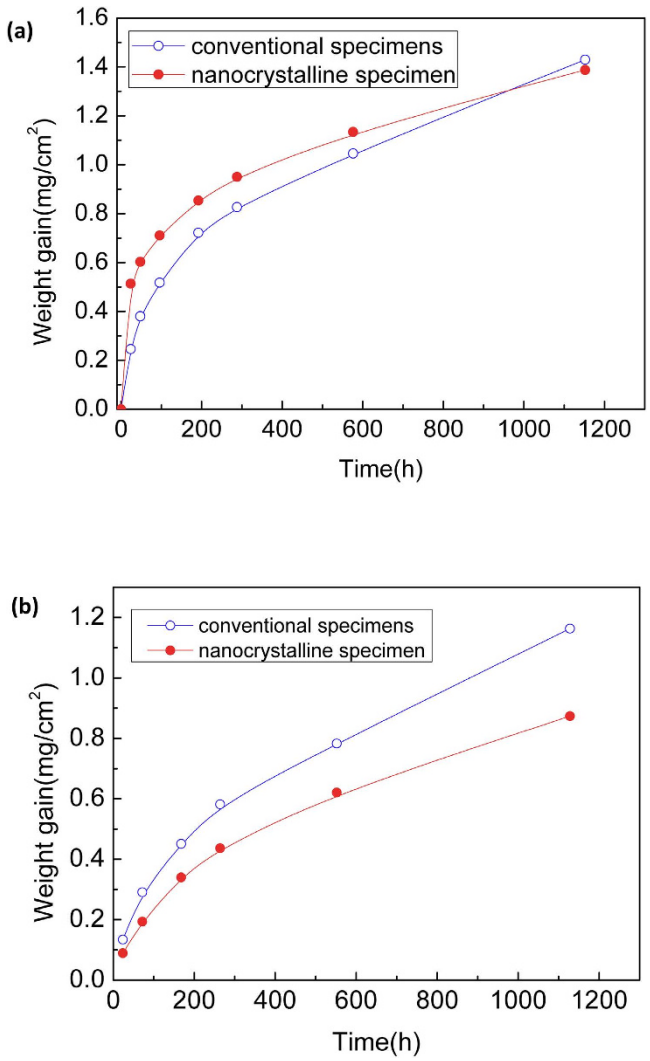

Figure 1. Oxidation kinetics of nanocrystalline and conventional specimens in water vapor with 848 K and 14.1 MPa. The parabola oxidation rate constant k is 0.044 in conventional specimens. However, the weight gain data (24 h) of the nanocrystalline specimens is not fitted to a parabola or a power law (**a**). The oxidation kinetics of the nanocrystalline exhibits parabolic law and oxidation rate constant k decreases to 0.026 after the data of 24 h oxidation is subtracted using the method of background subtraction (**b**).

provide theoretical supports for the improvement of oxidation behavior in heat resistant steels exposed to high-temperature and high-pressure water vapor.

The chemical composition of commercial P91 steel used in the present work is 0.1 C-0.6 Mn-8.8 Cr-0.95 Mo. A polished plate specimen (Φ50 mm × 4.0 mm in size) of a tempered P91 steel with conventional grain size of 14 μm was subjected to SMAT. SMAT was performed only on one side of the specimens. The set-up and procedure were described as follows: hardened 0.8 C steel balls, with 5 mm in diameter and mirror-like surfaces, were placed in a reflecting chamber that was vibrated by a vibration generator with a frequency of 20 kHz. After being treated for 30 min, the surface roughness of SMAT-ed sample is comparable to that of the original, unpolished specimen. Other details of the experimental setup and the SMAT processing are described in the reference[12].

In order to make comparisons of the oxidation resistance between convertional materials and SMAT-ed nanocrystalline materials, oxidation specimens with $10 \times 20 \times 2\,mm^3$ were cut by an electrical discharge machine for the nanocrystalline specimens and conventional grain specimens. The surfaces of specimens, except for the SMAT treated surface, were polished to mirror-like surface by 2.5 μm Al_2O_3 polishing paste, then cleaned in distilled water and then in acetone with ultrasonic agitation for 15 min prior to oxidation. Oxidation behaviors were tested in supercritical water oxidation equipments operated at 848 K and 14.1 MPa, and the total time of oxidation was up to 48 days (1152 h). Each oxidation date at different time was calculated by averaging the value from three specimens. Oxide scale were characterized by SEM, EPMA, XRD and TEM. Cross-sectional morphologies of the specimens were observed by using SEM with back-scattered electron (BSE) and Electron probe micro-analyzer (EPMA).

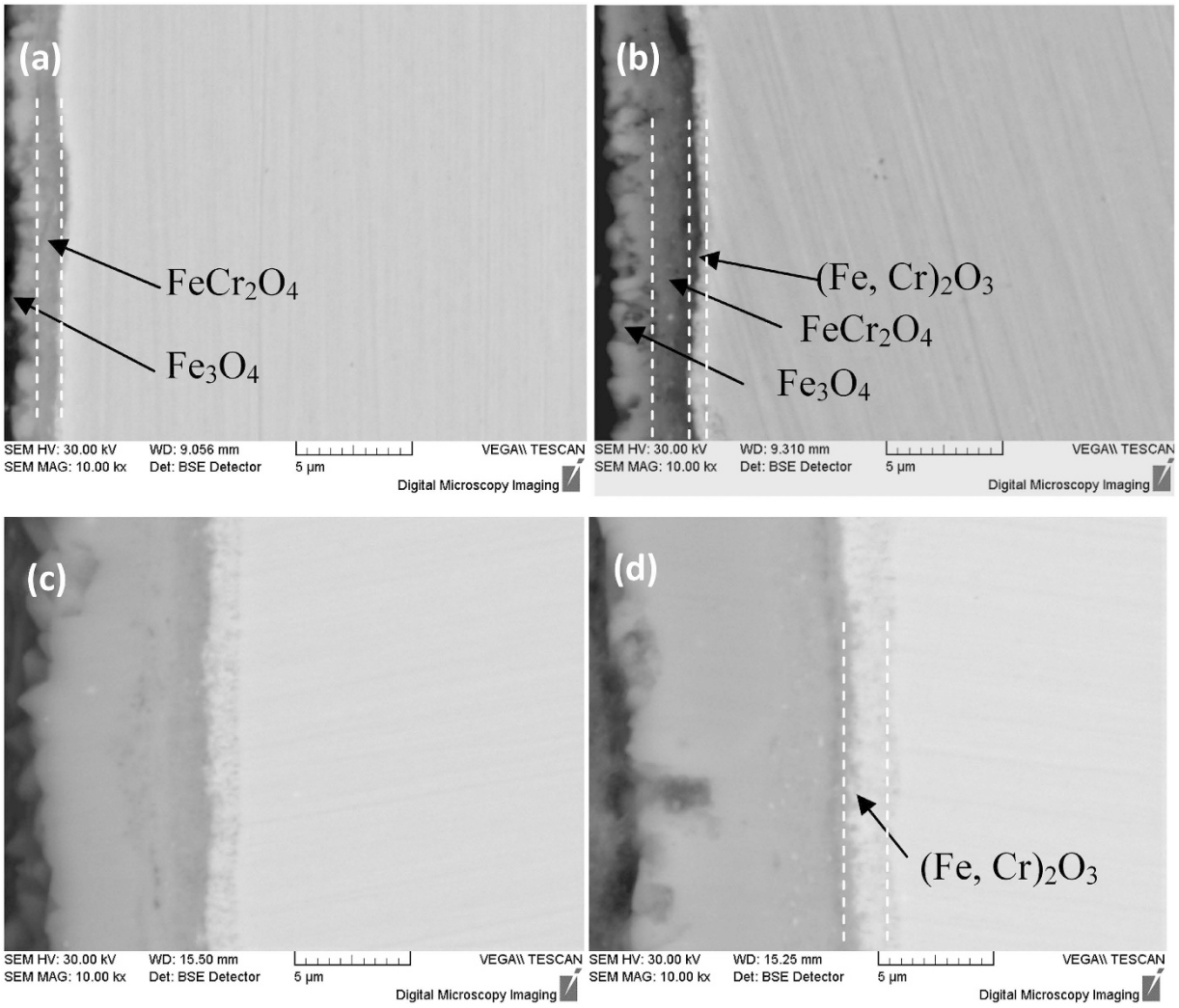

Figure 2. Cross-section back-scattered electron images of the oxide scale formed on the nanocrystalline surface layer exposure at 848 K. (**a**) after 24 h, (**b**) after 96 h, (**c**) after 576 h, (**d**) after 1152 h. The three-layer oxide structure from surface towards matrix is Fe_3O_4, spinel $FeCr_2O_4$ and corundum $(Fe,Cr)_2O_3$, The continuous $(Fe,Cr)_2O_3$ inner layer forms on the nanocrystalline surface layer of P91 steel at 848 K for 24 h.

Microstructure characterizations of nanocrystalline microstructure were also examined using TEM. Thin foil specimens for TEM observation were prepared using Focused Ion Beam instrument (FIB).

It is reported that the grains in the surface layer region within 100 μm thick are refined into nanometer scale, and the thermal stability of nanocrystalline microstructure is excellent until the temperature above 1033 K[7]. The time dependence of weight gain was plotted as a function of time in Fig. 1. The weight gain data of the conventional specimens were fitted to the parabola law relation given in Eq. (1):

$$\Delta W = kt^{1/2} \tag{1}$$

Where W is the weight gain in mg/cm^2, k is the oxidation rate constant in mg/cm^2/h, and t is time in hour. The oxidation rate constant k is 0.044 for the conventional specimens. However, the weight gain data (24 h) of the nanocrystalline specimens could not fitted to the parabola or a power law in Fig. 1a. Because the diffusivity of Cr in the nanocrystal grain is 4–5 orders of magnitude higher than that in the conventional grain[12] , both the diffusivity of oxygen and iron sharply increase in the nanocrystalline P91 steel. Therefore, P91 steel with nanocrystalline microstructure rapidly forms a double layer of Fe_3O_4 and $FeCr_2O_4$, and this will lead to an acceleration of the oxidation rate in the early stage before the formation of a more protective Cr-rich $(Fe, Cr)_2O_3$ oxide scale as shown in Fig. 2a. The data analysis of weight gain was considered as a starting from the 24 h oxidation specimen, the oxidation kinetics of the nanocrystalline exhibited parabolic law after the formation of the $(Fe, Cr)_2O_3$ inner layer on the nanocrystalline surface layer of P91 steel as shown in Fig. 2b–d, which causes a decreasing in the oxidation rate constant k from 0.044 in the conversional specimen to 0.026 in the nanocrystalline specimen (Fig. 1b), and this denotes a notable improvement of oxidation resistance on the nanocrystalline surface layer.

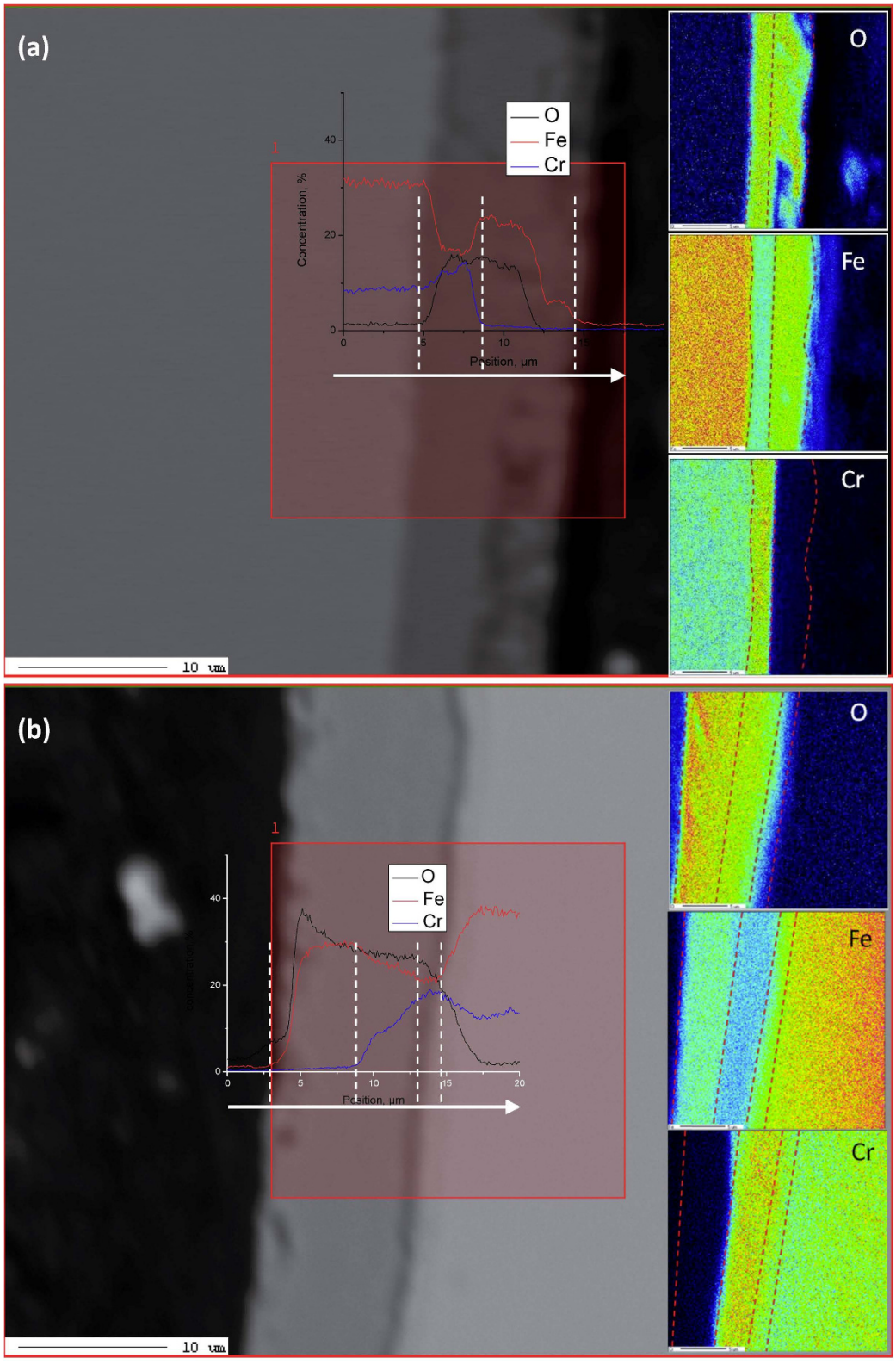

Figure 3. Chemical composition profiles of oxide scale formed on both the conventional (**a**) and nanocrystalline (**b**) specimens surface layer exposure at 848 K for 1152 h are performed using EPMA map/line-scan technique. The three-layer oxide structure from surface towards matrix was Fe_3O_4, spinel $FeCr_2O_4$ and corundum $(Fe,Cr)_2O_3$ formed on the nanocrystalline surface layer (**b**), it is different from the typical two-layer scale consisted of Fe_3O_4 outer layer and $FeCr_2O_4$ inner layer in conventional P91 steel (**a**). The inner oxide scale $(Cr, Fe)_2O_3$ is rich in Cr, which can be clearly seen from the cross-sectional scale morphology of the nanocrystalline surface layer.

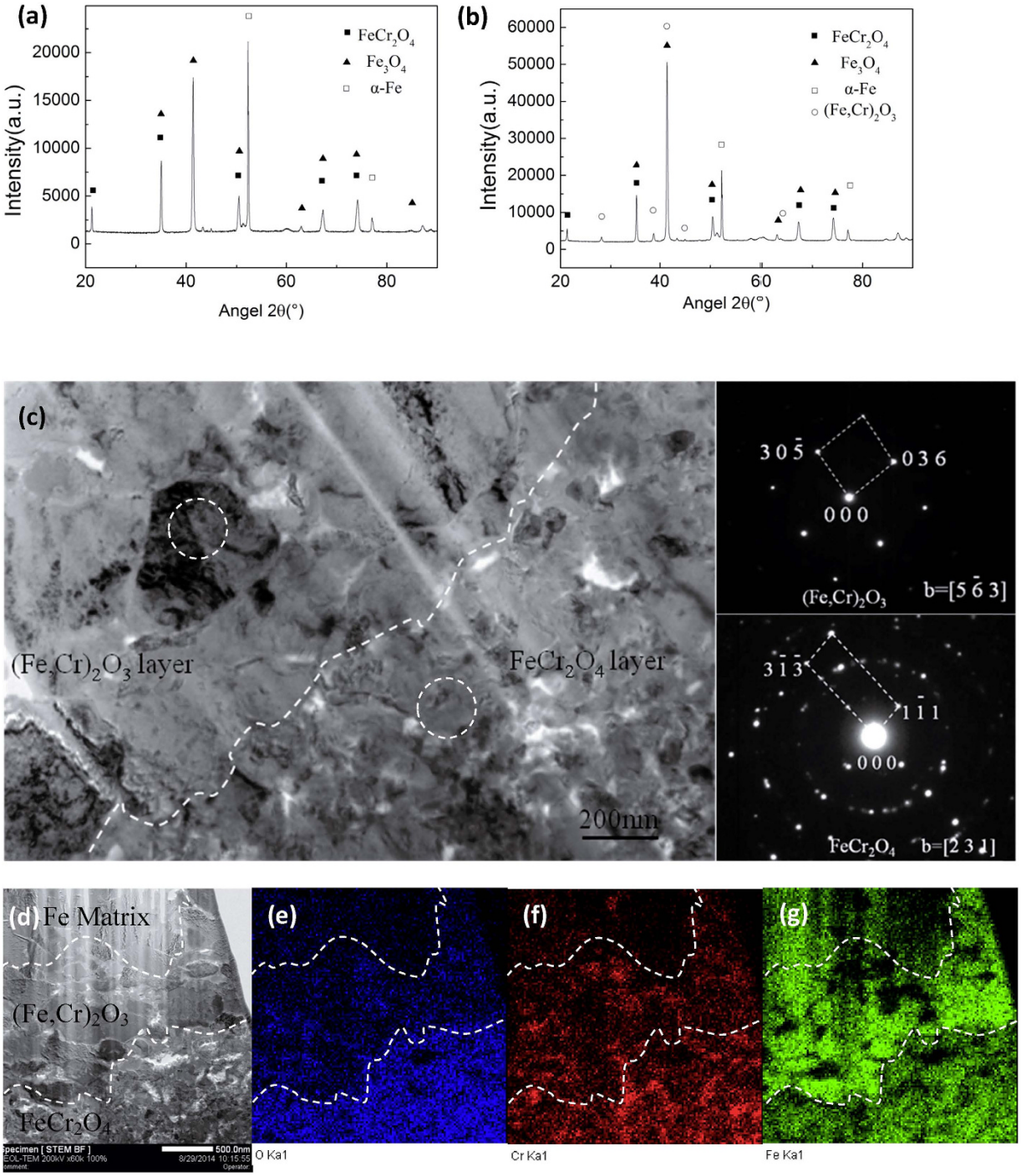

Figure 4. XRD patterns and TEM observation of the oxide scale formed on the nanocrystalline surface layer exposure at 848 K for 576 h. Fe_3O_4, $FeCr_2O_4$ were detected in the conventional specimen by XRD (**a**), Fe_3O_4, $FeCr_2O_4$ and (Cr, Fe)$_2O_3$.were detected in the nanocrystalline specimen by XRD (**b**). A bright-field TEM image and the electron diffraction pattern show the middle oxide scale and the inner scale are identified as $FeCr_2O_4$ and $(Fe,Cr)_2O_3$, respectively (**c**). The map-scan profiles also prove that the inner oxide scale (Cr, Fe)$_2O_3$ is rich in Cr (**d–g**).

To verify the results on the formation of (Fe, Cr)$_2O_3$, the chemical composition profiles of the oxide scale on both the conventional and the nanocrystalline specimens were examined using EPMA map/line-scan technique, as shown in Fig. 3. The oxide layer needs to be thick enough for EPMA analysis, so specimens exposed after 1152 h were selected. The three-layer oxide structure from the surface towards the alloy consisted of an Fe_3O_4 outer layer, a spinel $FeCr_2O_4$ in the middle, and a corundum (Fe, Cr)$_2O_3$

inner layer at the oxide/alloy interface. This is different from the typical two-layer scale consisting of an Fe_3O_4 outer layer and an $FeCr_2O_4$ inner layer on the conventional surface of P91 steel[13,14]. The O, Cr and Fe concentrations in the Fe_3O_4 and $FeCr_2O_4$ are similar in both the conventional and nanocrystalline specimens. However, the inner oxide scale $(Cr, Fe)_2O_3$ is richer in Cr, which can be clearly seen from the cross-sectional scale morphology in Fig. 3b. The XRD profiles of the conventional and nanocrystalline specimens exposed after 576 h are shown in Fig. 4a,b, respectively. Fe_3O_4, $FeCr_2O_4$ and $(Fe, Cr)_2O_3$ were all detected. Further analysis was performed using TEM to verify the morphology and phase structure of different types of oxides. The nanocrystalline specimen exposed after 576 h was selected to prepare the TEM foils because of the processing depth limitation in the FIB instrument. The selected area electron diffraction pattern (SAED) of TEM indicated that the oxide contained the spinel $FeCr_2O_4$ and the corundum $(Fe, Cr)_2O_3$ in Fig. 4c. The Cr concentration increased from 14.5 wt% in $FeCr_2O_4$ to 31.4 wt% in $(Fe, Cr)_2O_3$. The map-scan profiles also proved that the inner oxide scale $(Fe, Cr)_2O_3$ is richer in Cr (Fig. 4d–g).

Cr diffusion in the metal matrix and oxide is not fast enough for a stable corundum $(Fe, Cr)_2O_3$ scale in 9 Cr steel to form at 848 K. The scales of 10 Cr steel typically consist of an outer Fe_3O_4 layer and an inner layer containing $(Fe, Cr)_3O_4$ at 923 K in $Ar + 50\%H_2O$[15]. A scale composed of Fe_2O_3, Fe_3O_4, and $(Fe, Cr)_3O_4$ is formed on P91 steel at 923 K in steam atmospheres, and it is still composed of Fe_3O_4 and $(Fe, Cr)_3O_4$ at 1073 K[16]. These reports are in good agreement with the results of the conventional P91 steel specimens in this work. Although, the tendency for Cr to be selectively oxidized becomes more pronounced as diffusion in the alloy becomes enhanced with increasing temperature, the Cr concentration in 9 Cr steel is still not sufficiently high to allow the formation of a more protective $(Fe, Cr)_2O_3$ layer. However, the scale is composed mainly of $(Fe, Cr)_2O_3$ on AISI 430 steel with 16.21 wt% Cr content at 923 K, and a layer of Cr_2O_3 is formed at 1073 K owing to the higher diffusion rate of Cr at this temperature than at 923 K[16]. In this work, A protective $(Fe, Cr)_2O_3$ layer could form on the nanocrystalline surface layer in P91 steel with 8.8 wt% Cr at 848 K.

The oxidation process of the nanocrystalline surface layer is divided into two stages, namely before and after the formation of a protective $(Fe, Cr)_2O_3$ layer. Before the formation of the $(Fe, Cr)_2O_3$ layer, the diffusivity of oxygen and iron sharply increase on the nanocrystalline surface layer of P91 steel. So oxidation rates of the nanocrystalline specimens are significantly accelerated in the initial stage. Increase of the oxidation rate with decreasing grain size is attributed to the larger grain-boundary area, which result in an increase in the short circuit diffusion paths[17].The similar results showed that SMAT had a negative effect on the corrosion resistance of Fe[18]. In contrast, after the formation of a protective $(Fe, Cr)_2O_3$ layer, due to its higher density of grain boundaries in the nanocrystalline surface layer, a higher flux of Cr goes towards the $(Fe, Cr)_2O_3$-the alloy interface, while the spinel $(Fe, Cr)_2O_3$ and $FeCr_2O_4$ layer inhabits Cr and O/Fe diffusion through it. Therefore, the $(Fe, Cr)_2O_3$ scale at the alloy-oxide interface has a higher concentration of Cr. O and Fe diffusivity would also decrease due to the formation of $(Fe,Cr)_2O_3$ inner layer in the nanocrystalline surface layer of P91 steel. The enhancement of Cr diffusion guarantee the stable growth of the Cr-rich $(Fe, Cr)_2O_3$ scale, which significantly improve oxidation resistance. Even a Cr_2O_3 scale may be formed at higher temperatures owing to the higher diffusion rate of Cr.

References

1. Xia, Z. X. *et al.* Improve creep properties of reduced activation steels by controlling precipitation behaviors. *Mater. Sci. Eng. A*. **545,** 91–96 (2012).
2. Xia, Z. X., Zhang, C. & Yang, Z. G. Control of precipitation behavior in reduced activation steels by intermediate heat treatment. *Mater. Sci. Eng. A*, **528,** 6764–6768 (2011).
3. Masuyama, F. History of Power Plants and Progress in Heat Resistant Steels. *ISIJ Int*. **41,** 612–625 (2001).
4. Sun, M. C., Wu, X. Q., Han E. H. & Rao J. C. Microstructural characteristics of oxide scales grown on stainless steel exposed to supercritical water. *Scripta Mater*. **61,** 996–999 (2009).
5. Ren, R. M., Chen, C. H., Luan, W. Z. & Yang, D. X. The effect of surface nanocrystallization on oxidation resistance of 1Crl7 stainless steel. *Trans. Mater. Heat treat*. **28,** 188–192 (2007).
6. Peng, X., Yan, J., Zhou, Y. & Wang, F. Effect of grain refinement on the resistance of 304 stainless steel to breakaway oxidation in wet air. *Acta Mater*. **53,** 5079–5088 (2005).
7. Xia Z. X., Zhang, C., Liu, W. B. & Yang, Z. G. Effect of surface mechanical attrition treatment on precipitation behaviors and ferrite grains in heat resisting steels. *ISIJ Int*. **54,** 1935–1942 (2014).
8. Gleither, H. Nanocrystalline materials. *Prog. Mater. Sci*. **33,** 223–315(1989).
9. Wang, Z. B., Lu, K., Wilde, G. & Divinski, S. V. Interfacial diffusion in Cu with a gradient nanostructured surface layer. *Acta Mater*. **58,** 2376–2386 (2010).
10. Tong, W. P., Tao, N. R., Wang, Z. B., Lu. J. & Lu, K. Nitriding Iron at Lower Temperatures. *Science* **299,** 686–688 (2003).
11. Li, X. Y., Wei, Y. J., Lu, L., Lu, K. & Gao, H. J. Dislocation nucleation governed softening and maximum strength in nano-twinned metals. *Nature* **464,** 877–880 (2010).
12. Wang, Z. B., Tao, N. R., Tong, W. P., Lu, J. & Lu, K. Diffusion of chromium in nanocrystalline iron produced by means of surface mechanical attrition treatment. *Acta Mater*. **51,** 4319–4329 (2003).
13. Tan, L., Yang, Y., Allen, T. R. Oxidation behavior of iron-based alloy HCM12A exposed in supercritical water. *Corros. Sci*. **48,** 3123–3138 (2006).
14. Ampornrat, P., Was, G. S. Oxidation of ferritic-martensitic alloys T91, HCM12A and HT-9 in supercritical water, *J. Nucl.Mater*. **371,** 1–17 (2007).
15. Żurek, J. *et al.* Anomalous temperature dependence of oxidation kinetics during steam oxidation of ferritic steels in the temperature range 550-650°C. *Corros. Sci*. **46,** 2301–2317 (2004).
16. Sánchez, L., Hierro, M. P., Pérez, F. J. Effect of Chromium Content on the Oxidation Behaviour of Ferritic Steels for Applications in Steam Atmospheres at High Temperatures. *Oxid. Met*. **71,** 173–186 (2009).

17. Singh Raman, R. K., Khanna, A. S., Tiwari, R. K. & Gnanamoorthy, J. B. Influence of Grain Size on the Oxidation Resistance of 21/4Cr-1Mo steel. *Oxid. Met.* **37,** 1–12 (1992).
18. Zhong, C., Hu, W. B., Jiang, Y. M., Deng, B. & Li J. Lower temperature aluminizing and its effect on improving corrosion resistance of iron treated by surface mechanical attrition treatment. *J. Coat. Technol. Res.* **8,** 107–116 (2011).

Acknowledgements
The authors thank Wang Z.B. for sample preparation.

Author Contributions
X.Z.X., Z.C. and Y.Z.G. wrote the main manuscript text. H.X.F. and L.W.B. prepare figures 3–4. All authors reviewed the manuscript.

Additional Information
Competing financial interests: The authors declare no competing financial interests.

How to cite this article: Xia, Z. X. *et al.* Improve oxidation resistance at high temperature by nanocrystalline surface layer. *Sci. Rep.* **5**, 13027; doi: 10.1038/srep13027 (2015).